Technical Note

1966-63

R. K. Crane

Coherent Pulse Transmission Through Rain

27 December 1966

Prepared under Electronic Systems Division Contract AF 19(628)-5167 by

Lincoln Laboratory
MASSACHUSETTS INSTITUTE OF TECHNOLOGY
Lexington, Massachusetts

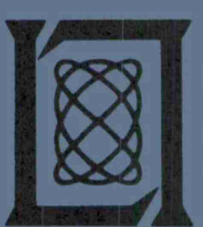

The work reported in this document was performed at Lincoln Laboratory, a center for research operated by Massachusetts Institute of Technology, with the support of the U.S. Air Force under Contract AF 19(628)-5167.

Distribution of this document is unlimited.

MASSACHUSETTS INSTITUTE OF TECHNOLOGY
LINCOLN LABORATORY

COHERENT PULSE TRANSMISSION THROUGH RAIN

R. K. CRANE

Group 61

TECHNICAL NOTE 1966-63

27 DECEMBER 1966

LEXINGTON MASSACHUSETTS

ABSTRACT

The problem of received signal degradation for coherent pulse transmission through a rain scattering volume was investigated for large bandwidth transmission at 4.0, 8.0, 15.5 and 34.86 GHz. Calculations of pulse length and total pulse energy were made for different path lengths through the rain volume. The calculations were made for models of heavy and extreme rainfall, using rain rates 49.0 and 196.3 mm/hr. The results of the computations show that for the rain rates considered, the dominant cause of signal degradation is attenuation. Negligible pulse lengthening was noted at 34.86 GHz. For rain rates above 196 mm/hr. and frequencies of 15.5 and 8.0 GHz, measurable values of pulse lengthening were calculated for bandwidths above 2.0 GHz. At 4.0 GHz, measurable values of pulse lengthening were obtained for both rain rates considered.

Accepted for the Air Force
Franklin C. Hudson
Chief, Lincoln Laboratory Office

Coherent Pulse Transmission Through Rain

I. INTRODUCTION

Electromagnetic transmission systems at microwave frequencies and higher are evolving toward the use of more and more bandwidth to carry more information. This study concentrates on a possible limitation to extremely wide bandwidth coherent transmission systems, the dispersion of rain scattering media. The study was conducted by considering a particular problem, the change in shape of a short pulse as it propagates through the rain-filled medium. Two models of a rain volume were used, one representative of heavy rain, the other of extremely heavy rain. These rain models were selected because it was anticipated that only at the extreme rain rates would pulse distortion be a problem. The results of the computations bear out the expectation. The major effect of rain scattering is to cause attenuation. At very large bandwidths, greater than 2 GHz, pulse lengthening gets to be larger than 2.0 percent for frequencies in the 4.0 to 15.5 GHz range for rain rates in excess of 196 mm/hr and propagation distances of the order of the largest distance possible in heavy rainstorms.

II. METHOD USED TO COMPUTE PULSE SHAPE

The shape of a pulse traveling through a dispersive medium is given by the Fourier integral theorem

$$\psi(t, \rho) = \int_{-\infty}^{\infty} \int_{-\infty}^{\infty} \psi(t', 0) \exp\{-i2\pi f[t' - t + n(f)\rho]\}\, dt'df$$

where $\psi(t, \rho)$ = a component of the electromagnetic field

t = time

$\rho = z/c$, z = distance, c = velocity of light

f = frequency

$n(f)$ = index of refraction of the medium

A transmitted waveform of this type

$$\psi(t, 0) = a(t, 0) \exp\{i2\pi f_c t\} \quad ,$$

has as its Fourier transform

$$\bar{\psi}(f, 0) = \int_{-\infty}^{\infty} a(t', 0) \exp\{-i2\pi(f - f_c)t'\}\, dt' = \bar{a}(f - f_c, 0)$$

$$= \bar{a}(\sigma, 0)$$

where $\sigma = f - f_c$, f_c = carrier frequency.

The resultant integral theorem for the frequency difference, σ, then is

$$\psi(t, \rho) = \int_{-\infty}^{\infty} \int_{-\infty}^{\infty} a(t', 0) \exp\{-i2\pi(f - f_c)\, t' + i2\pi(f - f_c)\, t + 2\pi f_c t - i2\pi f n(f)\rho\}\, dt'df$$

$$= e^{i2\pi f_c t} \int_{-\infty}^{\infty} \bar{a}(\sigma, 0) \exp\{i2\pi\sigma t - i2\pi\rho\varphi(\sigma)\}\, d\sigma$$

$$= a(t, \rho) \exp\{i2\pi f_c t\} \quad .$$

The pulse shape used for this analysis was taken to have a truncated Gaussian spectrum

$$\bar{a}(\sigma, 0) = \exp\{-\pi(\frac{\sigma}{\sigma_o})^2\}, \quad |\sigma| \leq |\sigma_m| = 2.5 \text{ GHz}$$

$$= 0, \quad |\sigma| > |\sigma_m| \quad .$$

Using this pulse shape and a power series expansion of the phase function about the carrier frequency, the equation for the pulse shape is

$$a(t, \rho) = \int_{-\sigma_m}^{+\sigma_m} \bar{a}(\sigma, 0) \exp\{-i 2\pi\rho \sum_{j=1}^{M} (A_j - iB_j)\sigma^{j-1} + - i 2\pi(f_c + \sigma)\rho + i 2\pi\sigma t\} d\sigma \quad .$$

This equation cannot be integrated by the usual approximate techniques for the region of interest, $t - A_2\rho$ and ρ small. In this region, the argument of the integral is well behaved and the integral can be readily computed using numerical techniques.

The total energy contained in the pulse is also computed as:

$$\varepsilon(\rho) = \int_{-\sigma_m}^{\sigma_m} \bar{a}^*(\sigma, 0)\, \bar{a}(\sigma, 0) \exp\{-4\pi\rho \sum_{j=1}^{M} B_j \sigma^{j-1}\} d\sigma \quad .$$

This integral can also be evaluated by the same techniques as for the pulse shape.

A numerical integration was performed using a sum of five-point Gaussian

quadrature integrations, each for a subinterval of the range $-\sigma_m$ to σ_m. The number of subintervals was chosen such that the pulse attenuation

$$\text{Att} = 10 \log_{10}[\varepsilon(\rho)/\varepsilon(0)]$$

varied by less than 0.01 percent for any further subdivision of the interval and such that the pulse shape, $a(t, \rho)$, varied by less than 0.01 percent as a function of time for a given distance over the values of time used to compute the pulse length.

III. DESCRIPTION OF THE SCATTERING MEDIUM

The phase function for the rain scattering medium was computed using an effective index of refraction for the medium. Both the real and imaginary parts of the effective index of refraction of the scattering medium were computed using Mie theory to calculate the effect of a single scatterer and then using single scattering theory to sum the effects of all the scatterers. The effective index of refraction is given by Van de Hulst.[1]

$$n_s = n_s' - i n_s'' = 1 - i \frac{2\pi}{k^3} \int_{a_{min}}^{a_{max}} S(n, a)\, N(a)\, da$$

where n_s = effective index of refraction of the medium

$k = \frac{2\pi}{\lambda}$ = wave number, λ = wavelength

$S(n, a)$ = single scattering amplitude in forward direction

n = index of refraction of scatterer

a = radius of scatterer

N(a) = number of density of scatterers in volume.

This index of refraction describes the change of the expected values of the field with distance through the medium. The use of this parameter to describe propagation through a medium requires the assumption that the expected value of the field variable is the quantity of interest. Transmission systems utilizing the expected value of the field are generally called coherent and, in this context, the results of this analysis are applicable to coherent transmission.

The index of refraction of the medium depends upon the electrical properties of the raindrops through the index of refraction of the water in the drop and the size distribution of the raindrops. The electrical properties of the liquid water were computed using the Debye formula and the values of the constants given in Kerr.[2] The model raindrop distributions used were taken from data obtained in Miami (Mueller)[3] and apply to convective storms. The 196.3 mm/hr rain model was taken from a least square fit of measured data to an assumed quadratic variation of the logarithm of liquid water content with drop radius. The 49.0 mm/hr rain model was taken as a biexponential curve fitting the average of five consecutive drop-size measurements. Both models are shown in Fig. 1 together with the data used to generate the 196.3 mm/hr model.

The maximum linear extent of the rain cells that would produce the modeled rain rates is of the order of 25 km for 49.0 mm/hr and 10 km for 196.3 mm/hr. The rainstorm models used for this study consist of assuming the rain rates and drop-size distributions are homogeneous through the entire storm volume and the rain drops are all at 18°C. These assumptions are required so that the effective index of refraction for the medium computed above will apply to all parts of the volume.

The calculated values of the index of refraction of the medium for different frequencies are given in Figs. 2 and 3. For calculations of pulse shape, it is convenient to have an analytical description of the variation of the index of refraction with frequency. The method used to describe this variation for the rain scattering medium was to expand the phase function in a power series about the carrier frequency.

$$\varphi = f\, n(f) = \sum_{j=1}^{M} (A_j - iB_j)\,(f - f_c)^{j-1} + f \quad .$$

The values A_j and B_j were found using a least square fit to calculated values of the phase function evaluated in frequency steps of 0.25 GHz about the center frequency. Twenty-one values were used for each curve fit. The A_j and B_j values for the two rainstorm models and the center frequencies of interest are given in Tables 1 and 2.

A rough estimate of the frequency band that will produce the maximum

distortion can be made using the refractivity and attenuation vs. frequency plots. The pulse shape equation may be rearranged to give

$$a(t, \rho) = \exp\{-i\,2\pi\rho\,(f_c + A_1 - iB_1)\} \int_{-\sigma_m}^{\sigma_m} \bar{a}\,(\sigma, o) \exp\{i\,2\pi\xi\} \times$$

$$\times \exp\{-2\pi i\rho \sum_{j=3}^{M} (A_j - iB_j)\,\sigma^{j-1}\}\,d\sigma$$

where $\xi = t - (1 + A_2 - iB_2)\rho$.

In this form it is evident that the only contribution to the change in shape of the pulse magnitude vs. time curve comes from the phase function terms with subscript higher than 2.

The attenuation coefficient is related to the phase function by

$$Att = \left[\frac{4\pi \log_{10} e}{c} \times 10^5\right] fn''(f) = \left[\frac{4\pi \log_{10} e}{c} \times 10^5\right] Im[\varphi(f)]$$

where c = velocity of light in cm/sec

Att = attenuation coefficient in db/km .

This means that any curvature evident in the attenuation coefficient vs. frequency curve will give rise to pulse distortion. Since the refractivity is related to the real part of this phase function divided by the frequency, the interpretation of this curve relies more upon locating higher order changes in curvature. From an examination of Figs. 2 and 3, it can be expected that

the maximum pulse distortion will occur in the 2 to 10 GHz frequency band. It is also expected that the distortion effects at the 196.3 mm/hr rain rate will far exceed those at the lower rain rate.

IV. RESULTS OF COMPUTATION

The parameters of interest for pulse propagation are the loss of total energy of the pulse and the change in pulse shape. The pulse shape is characterized by a pulse length that is taken as the time delay between points on the pulse magnitude curve that are at 0.707 times the maximum pulse magnitude. The bandwidth of the pulse is also taken as the reciprocal of this pulse length. The pulse length was determined from plots of the pulse magnitude showing values of time either side of the peak value. Typical pulse magnitude curves are shown in Fig. 4. In this figure the magnitude of $a(t, \rho)$ is given for different values of path length and transmitted pulse width.

The pulse length was computed as a percent of the transmitted pulse length. The accuracy of the pulse length computation depends upon the method used to locate the peak of the pulse and the slope of the pulse magnitude curve at the 0.707 point. The peak was taken as the highest value of the set of points calculated. In each case, the position of the peak may be off by as much as one-half a time interval. Referring to the pulse magnitude curves, the change in pulse height over this interval can be as much as 0.5 percent. This can cause a maximum error of about one-sixth a time interval in finding pulse length, or an error of less than 1.3 percent. The calculations of both

pulse length and pulse attenuation are given in Tables 3 to 6.

In general, the results show that the prime cause of signal degradation is attenuation. The monochromatic attenuation for the carrier frequency is 146 dB for 15.5 GHz and 384 dB for 34.86 GHz for the higher rate and the 10 km path. The pulse attenuation for low values of bandwidth is identical to the monochromatic attenuation. For a 3.64 GHz bandwidth at 15.5 GHz the decrease in pulse attenuation was only 9 dB, resulting in an overall loss of 137 dB. These large losses far overshadow the changes in pulse width that occur and in currently practical systems, the rain medium does not constitute a bandwidth limitation to coherent transmission systems.

For the two lower frequency bands considered, 4.0 and 8.0 GHz, attenuation does not limit pulse transmission so severely. The total pulse attenuation is only 32.7 for the 8.0 GHz carrier and 2.37 dB for the 4.0 GHz carrier at the higher rain rate, for 3.64 GHz bandwidth, and a 10 km path length. The percent pulse length increase for these two cases are 57 and 12, respectively. For the lower rain rate 25.0 km and the same bandwidth, the results give 26.6 dB pulse attenuation and 10 percent pulse length increase for a 8.0 GHz carrier and 3.0 dB pulse attenuation and 14 percent pulse length increase for a 4.0 GHz carrier.

The percent pulse length change, distance variation, is depicted in Figs. 5 to 7 for the cases for which the change exceeds 2 percent. It is noted that for the larger bandwidths and carrier frequencies of 8.0 GHz and 15.5 GHz, the change of percent pulse length change gets larger with increasing band-

width after a particular value of range or a critical distance is reached. The pulse attenuation results for these bands further show that after the critical distance is reached the pulse attenuation curve deviates markedly from the monochromatic attenuation curve. The critical distance can be considered the distance at which the pulse begins to distort. This distance decreases with increasing bandwidth. Using a critical distance criterion for the onset of pulse distortion, the results show that for both 8.0 and 15.5 GHz, distortion occurs within 5 km for bandwidths in excess of 3.0 GHz and the higher rain rate.

V. APPLICATION TO STORM MODELS

The computations given above are for an idealized storm situation, a homogenous drop distribution, and an 18.0°C drop temperature. Reasonable models of severe storms show that the rain rates vary strongly throughout the storm and the drop temperatures decrease from a high surface value to freezing. Computations of possible pulse distortion should allow for variations in both drop distributions and temperature.

If the drop-size distributions are assumed to vary only slightly over the first Fresnel zone, the phase function, distance product can be replaced by a line integral as

$$a(t, \frac{z}{c}) = \int_{-\infty}^{\infty} \bar{a}(\sigma, 0) \exp\left\{i2\pi\sigma t - i\frac{2\pi f}{c}\int_{0}^{z} n(f, x)\, dx\right\} d\sigma \quad .$$

The criterion for distortion can then be replaced by the requirement that the rain rate exceed 196.3 mm/hr for a total of 5 km along the path. For the maximum storm distances considered, the Fresnel zone criterion requires the rain rates to be homogeneous over distances of the order of 20 meters.

The variation of the critical distance with drop temperature was investigated in the same manner as above. For drop temperatures lower than 18°C the results show a smaller amount of pulse distortion for both rain rates and all frequencies. The results of computations for the 30°C drop temperature show that the maximum distortion occurs for a 8.0 GHz carrier. At this frequency a pulse change of 80 percent for 10 km distance and a 3.0 GHz bandwidth, 40 percent change for 10 km for 2.26 GHz bandwidth and a critical distance less than 2 km for bandwidths in excess of 2.0 GHz resulted.

VI. CONCLUSIONS

The results of pulse length and pulse attenuation computations for wideband transmission through extreme rain rates show that for carrier frequencies above 10.0 GHz the problem is mainly one of attenuation, the critical distances for pulse distortion corresponding to attenuation above 100 dB. The situation at the lower carrier frequencies is not so severe and measurable pulse lengthening is possible. For storms in temperate climates, where drop temperatures do not exceed 18°C for large distances along the propagation path, bandwidths in excess of 3.6 GHz must be used before pulse distor-

tion becomes important. For climates where path lengths may be as large as 2 to 3 km with drop temperatures above 30.0°C, pulse distortion is a possible problem for bandwidths larger than 2.0 GHz.

REFERENCES

1. H. C. Van de Hulst, "Light Scattering by Small Particles" (J. Wiley and Sons, New York, 1957). Chapter 4.

2. D. E. Kerr, "Propagation of Short Radio Waves" (Mc-Graw-Hill, New York, 1951).

3. E. A. Mueller, "Raindrop Distributions at Miami, Florida," Research Report No. 9B, Illinois State Water Survey Meteorological Laboratory, University of Illinois, Urbana, Illinois (1959).

TABLE 1

EXPANSION COEFFICIENTS FOR THE PHASE FUNCTION

(49.0 mm/hr Drop Model, 18.0°C Drop Temperature)

FREQUENCY GHz	A_1 cps	A_2 cps/GHz	A_3 cps/GHz^2	A_4 cps/GHz^3	A_5 cps/GHz^4
4.0	10504.0	2992.7	−74.94	−54.54	3.969
8.0	19387.2	1471.9	−129.9	−12.93	−1.074
15.5	25964.8	463.2	−51.10	−1.897	−0.181
24.0	25414.3	−569.8	−45.92	−2.224	−0.022
34.86	16585.5	−833.4	14.11	0.943	−0.055
FREQUENCY GHz	B_1 cps	B_2 cps/GHz	B_3 cps/GHz^2	B_4 cps/GHz^3	B_5 cps/GHz^4
4.0	803.81	991.57	351.36	−5.125	−14.83
8.0	7724.2	1910.8	−19.43	−5.444	1.774
15.5	21091.6	1731.2	6.428	0.581	0.409
24.0	35192.9	1409.4	−46.91	−1.242	0.103
34.86	44535.7	354.3	−36.83	1.245	0.014

TABLE 2

EXPANSION COEFFICIENTS FOR THE PHASE FUNCTION (Cont.)

(196.3 mm/hr Drop Model, 18.0°C Drop Temperature)

FREQUENCY GHz	A_1 cps	A_2 cps/GHz	A_3 cps/GHz^2	A_4 cps/GHz^3	A_5 cps/GHz^4
4.0	42149.5	12432.8	812.9	−16.39	−42.78
8.0	90898.5	7030.4	−1640.3	175.9	49.48
15.5	128228.5	5057.0	−233.4	−41.04	1.919
24.0	141361.1	−2099.5	−322.5	19.90	0.209
34.86	102721.7	−3607.1	64.29	1.850	−0.277
FREQUENCY GHz	B_1 cps	B_2 cps/GHz	B_3 cps/GHz^2	B_4 cps/GHz^3	B_5 cps/GHz^4
4.0	1033.6	1097.7	617.02	208.04	29.44
8.0	27487.1	10363.6	−531.7	−274.9	62.01
15.5	80393.4	7768.9	351.1	−7.749	−3.767
24.0	156493.4	8147.5	−278.4	−11.40	1.316
34.86	210962.1	2479.9	−154.1	6.910	−0.165

TABLE 3

Pulse Length Change and Attenuation

4.0 GHz Center Frequency — 18°C Drop Temperature

49.0 mm/hr Drop Model						193.3 mm/hr Drop-Size Model			
Bandwidth GHz	Distance km	Pulse Length ns	Percent Change	Pulse Atten. dB	Monopulse A dB	Pulse Length ns	Percent Change	Pulse Atten. dB	Monopulse A dB
0.753	Trans.	1.328	-	-	-	1.328	-	-	-
	1.0	1.328	0.0	.1475	0.0005	1.328	0.0	0.1904	0.0025
	2.5	1.329	0.075	.3685	0.0015	1.329	0.075	0.4756	0.0065
	5.0	1.330	0.151	.7361	0.0039	1.331	0.226	0.9500	0.0143
	10.0	1.332	0.301	1.469	0.0110	1.335	0.527	1.895	0.0335
	25.0	1.337	0.678	3.644	0.0560	-	-	-	-
1.506	Trans.	0.6639	-	-	-	0.6639	-	-	-
	1.0	0.6646	0.105	.1511	-0.0031	0.6653	0.211	0.1969	-0.0041
	2.5	0.6657	0.271	.3765	-0.0065	0.6674	0.527	0.4906	-0.0085
	5.0	0.6676	0.557	.7493	-0.0093	0.6710	1.069	0.9761	-0.0119
	10.0	0.6714	1.130	1.484	-0.0040	0.6783	2.169	1.933	-0.0045
	25.0	0.6827	2.832	3.605	0.0950	-	-	-	-
2.259	Trans.	0.4426	-	-	-	0.4426	-	-	-
	1.0	0.4437	0.244	.1568	-0.0088	0.4449	0.520	0.2078	-0.0150
	2.5	0.4453	0.610	.3895	-0.0195	0.4482	1.265	0.5154	-0.0333
	5.0	0.4480	1.220	.7706	-0.0306	0.4538	2.531	1.018	-0.0538
	10.0	0.4534	2.440	1.509	-0.0290	0.4649	5.038	1.989	-0.0605
	25.0	0.4694	6.055	3.551	0.1490	-	-	-	-
2.996	Trans.	0.3338	-	-	-	0.3338	-	-	-
	1.0	0.3351	0.389	.1646	-0.0166	0.3368	0.899	0.2232	-0.0304
	2.5	0.3371	0.989	.4069	-0.0369	0.3413	2.247	0.5497	-0.0676
	5.0	0.3404	1.977	.7990	-0.0590	0.3485	4.404	1.073	-0.1088
	10.0	0.3471	3.984	1.542	-0.0620	0.3625	8.598	2.056	-0.1275
	25.0	3.668	9.886	3.495	0.2050	-	-	-	-
3.635	Trans.	0.2751	-	-	-	0.2751	-	-	-
	1.0	0.2765	0.509	.1740	-0.0260	0.2785	1.236	0.2431	-0.0503
	2.5	0.2786	1.272	.4279	-0.0579	0.2833	2.981	0.5922	-0.1101
	5.0	0.2821	2.545	.8329	-0.0929	0.2913	5.889	1.139	-0.1748
	10.0	0.2894	5.198	1.581	-0.1010	0.3073	11.71	2.128	-0.1995
	25.0	0.3123	13.52	3.442	0.2580	-	-	-	-

TABLE 4

Pulse Length Change and Attenuation

8.0 GHz Center Grequency 18°C Drop Temperature

49.0 mm/hr Drop Model						196.3 mm/hr Drop Model			
Band-width GHz	Distance km	Pulse Length ns	Percent Change	Pulse Atten. dB	Mono-pulse A dB	Pulse Length ns	Percent Change	Pulse Atten. dB	Mono-pulse A dB
0.753	Trans.	1.328	-	-	-	1.328	-	-	-
	1.0	1.328	0.0	1.406	0.000	1.327	-0.075	4.994	0.015
	2.5	1.328	0.0	3.513	0.002	1.326	-0.151	12.45	0.073
	5.0	1.328	0.0	7.023	0.008	1.325	-0.226	24.81	0.235
	10.0	1.327	-0.075	14.03	0.031	1.323	-0.377	49.20	0.890
	25.0	1.327	-0.075	34.98	0.173	-	-	-	-
1.506	Trans.	0.6639	-	-	-	0.6639	-	-	-
	1.0	0.6638	0.0	1.405	0.001	0.6629	-0.151	4.964	0.045
	2.5	0.6638	0.0	3.508	0.007	0.6619	-0.301	12.29	0.233
	5.0	0.6637	-0.030	7.002	0.029	0.6614	-0.377	24.16	0.885
	10.0	0.6635	-0.060	13.95	0.101	0.6668	0.437	46.66	3.43
	25.0	0.6632	-0.105	34.45	0.703	-	-	-	-
2.259	Trans.	0.4426	-	-	-	0.4426	-	-	-
	1.0	0.4426	0.0	1.403	0.003	0.4416	-0.226	4.916	0.093
	2.5	0.4425	-0.023	3.498	0.017	0.4415	-0.248	12.01	0.513
	5.0	0.4424	-0.045	6.965	0.066	0.4464	0.859	23.11	1.935
	10.0	0.4423	-0.068	13.81	0.251	0.4698	6.146	42.51	7.58
	25.0	0.4430	0.090	33.58	1.57	-	-	-	-
2.996	Trans.	0.3338	-	-	-	0.3338	-	-	-
	1.0	0.3338	0.0	1.401	0.005	0.3333	-0.150	4.851	0.158
	2.5	0.3338	0.0	3.485	0.030	0.3363	0.749	11.65	0.873
	5.0	0.3339	0.030	6.915	0.116	0.3510	5.153	21.70	3.35
	10.0	0.3346	0.240	13.61	0.471	0.4168	25.87	37.44	12.65
	25.0	0.3424	2.576	32.35	2.80	-	-	-	-
3.635	Trans.	0.2751	-	-	-	0.2751	-	-	-
	1.0	0.2751	0.0	1.398	0.008	0.2756	0.182	4.774	0.235
	2.5	0.2752	0.036	3.469	0.046	0.2834	3.017	11.22	1.303
	5.0	0.2759	0.291	6.852	0.179	0.3158	14.80	20.11	4.435
	10.0	0.2789	1.381	13.36	0.701	0.4322	57.11	32.71	17.37
	25.0	0.3019	9.742	30.85	4.30	-	-	-	-

TABLE 5

Pulse Length Change and Attentuation

15.5 GHz Center Frequency 18°C Drop Temperature

		49.0 mm/hr Drop Model				196.3 mm/hr Drop Model			
Band-width GHz	Distance km	Pulse Length ns	Percent Change	Pulse Atten. dB	Mono-pulse A dB	Pulse Length ns	Percent Change	Pulse Atten. dB	Mono-pulse A dB
0.753	Trans.	1.328	-	-	-	1.328	-	-	-
	1.0	1.328	0.0	3.839	0.000	1.328	0.0	14.63	0.01
	2.5	1.328	0.0	9.598	0.001	1.329	0.075	36.56	0.03
	5.0	1.328	0.0	19.19	0.01	1.330	0.151	73.06	0.12
	10.0	1.328	0.0	38.37	0.02	1.332	0.310	145.9	0.5
	25.0	1.328	0.0	95.85	0.14	-	-	-	-
1.506	Trans.	0.6639	-	-	-	0.6639	-	-	-
	1.0	0.6639	0.0	3.839	0.000	0.6646	0.105	14.62	0.02
	2.5	0.6639	0.0	9.594	0.005	0.6658	0.286	36.48	0.11
	5.0	0.6639	0.0	19.18	0.02	0.6678	0.587	72.74	0.44
	10.0	0.6640	0.015	38.31	0.08	0.6717	1.175	144.6	1.8
	25.0	0.6642	0.045	95.43	0.56	-	-	-	-
2.259	Trans.	0.4426	-	-	-	0.4426	-	-	-
	1.0	0.4426	0.0	3.838	0.001	0.4438	0.271	14.60	0.04
	2.5	0.4427	0.023	9.587	0.012	0.4455	0.655	36.36	0.23
	5.0	0.4427	0.023	19.15	0.04	0.4486	1.356	72.22	0.96
	10.0	0.4428	0.045	38.19	0.21	0.4550	2.802	142.5	3.9
	25.0	0.4438	0.158	94.72	1.27	-	-	-	-
2.996	Trans.	0.3338	-	-	-	0.3338	-	-	-
	1.0	0.3339	0.030	3.836	0.003	0.3354	0.479	14.58	0.06
	2.5	0.3339	0.030	9.577	0.022	0.3384	1.378	36.19	0.40
	5.0	0.3341	0.090	19.11	0.09	0.3449	3.325	71.52	1.66
	10.0	0.3349	0.330	38.04	0.36	0.3650	9.347	139.9	6.5
	25.0	0.3400	1.857	93.73	2.26	-	-	-	-
3.635	Trans.	0.2751	-	-	-	0.2751	-	-	-
	1.0	0.2752	0.036	3.835	0.004	0.2773	0.800	14.55	0.09
	2.5	0.2754	0.109	9.565	0.034	0.2827	2.763	35.98	0.61
	5.0	0.2760	0.327	19.06	0.14	0.2968	7.888	70.68	2.5
	10.0	0.2786	1.272	37.84	0.56	0.3445	25.23	136.9	9.5
	25.0	0.2790	7.597	92.51	3.48	-	-	-	-

TABLE 6

Pulse Length Change and Attenuation

34.86 Center Frequency 18°C Drop Temperature

49.0 mm/hr Drop Model						196.3 mm/hr Drop Model			
Bandwidth GHz	Distance km	Pulse Length ns	Percent Change	Pulse Atten. dB	Monopulse A dB	Pulse Length ns	Percent Change	Pulse Atten. dB	Monopulse A dB
0.753	Trans.	1.328	-	-	-	1.328	-	-	-
	1.0	1.328	0.0	8.107	0.000	1.328	0.0	38.41	0.0
	2.5	1.328	0.0	20.27	0.00	1.327	-0.075	96.02	0.0
	5.0	1.327	-0.075	40.54	0.00	1.327	-0.075	192.0	0.0
	10.0	1.327	-0.075	81.07	0.00	1.326	-0.151	384.1	0.0
	25.0	1.327	-0.075	202.7	0.0	-	-	-	-
1.506	Trans.	0.6639	-	-	-	0.6639	-	-	-
	1.0	0.6638	-0.015	8.107	0.000	0.6635	-0.060	38.41	0.0
	2.5	0.6637	-0.045	20.27	0.00	0.6630	-0.136	96.01	0.01
	5.0	0.6634	-0.075	40.54	0.00	0.6621	-0.271	192.0	0.0
	10.0	0.6630	-0.136	81.07	0.00	0.6604	-0.527	383.9	0.2
	25.0	0.6618	-0.316	202.6	0.1	-	-	-	-
2.259	Trans.	0.4426	-	-	-	0.4426	-	-	-
	1.0	0.4425	-0.023	8.107	0.000	0.4421	-0.113	38.40	0.01
	2.5	0.4423	-0.068	20.27	0.00	0.4413	-0.294	95.99	0.02
	5.0	0.4420	-0.136	40.53	0.01	0.4400	-0.587	191.9	0.1
	10.0	0.4414	-0.271	81.05	0.02	0.4374	-1.175	383.6	0.5
	25.0	0.4395	-0.700	202.6	0.1	-	-	-	-
2.996	Trans.	0.3338	-	-	-	0.3338	-	-	-
	1.0	0.3337	-0.030	8.105	0.002	0.3332	-0.180	38.39	0.02
	2.5	0.3335	-0.090	20.26	0.01	0.3323	-0.449	95.96	0.06
	5.0	0.3331	-0.210	40.52	0.02	0.3310	-0.839	191.8	0.2
	10.0	0.3323	-0.449	81.03	0.04	0.3291	-1.408	383.2	0.9
	25.0	0.3301	-1.108	202.5	0.2	-	-	-	-
3.635	Trans.	0.2751	-	-	-	0.2751	-	-	-
	1.0	0.2750	-0.036	8.103	0.004	0.2745	-0.218	38.39	0.02
	2.5	0.2747	-0.145	20.25	0.02	0.2738	-0.473	95.92	0.10
	5.0	0.2743	-0.281	40.50	0.04	0.2733	-0.654	191.7	0.3
	10.0	0.2736	-0.545	81.00	0.07	0.2756	+0.182	382.7	1.4
	25.0	0.2718	-1.200	202.3	0.4	-	-	-	-

3-61-4759

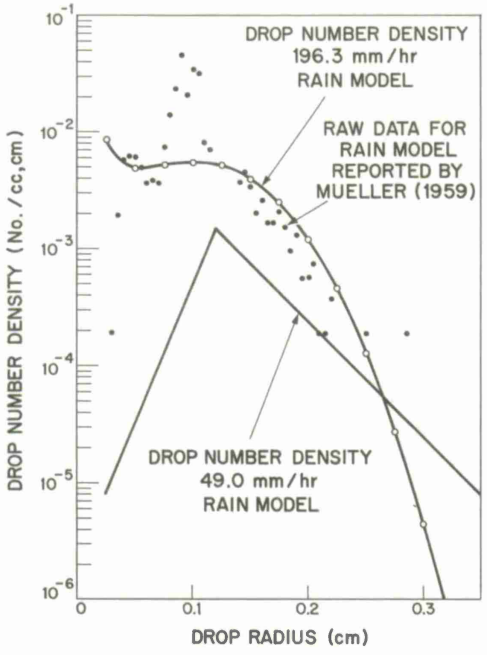

Fig. 1. Drop number density vs. drop radius.

3-61-4750

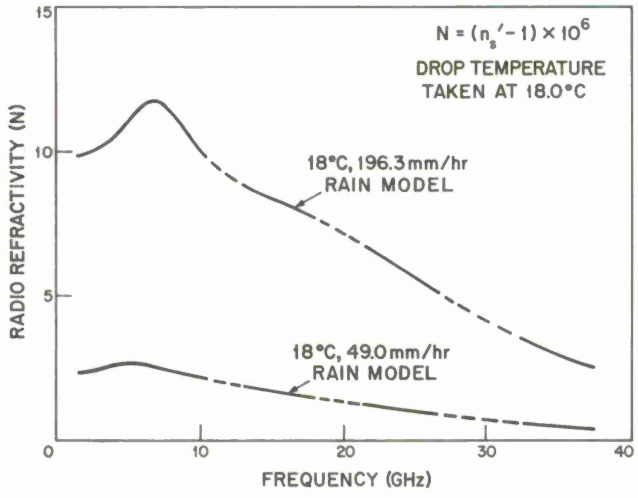

Fig. 2. Radio refractivity vs. frequency.

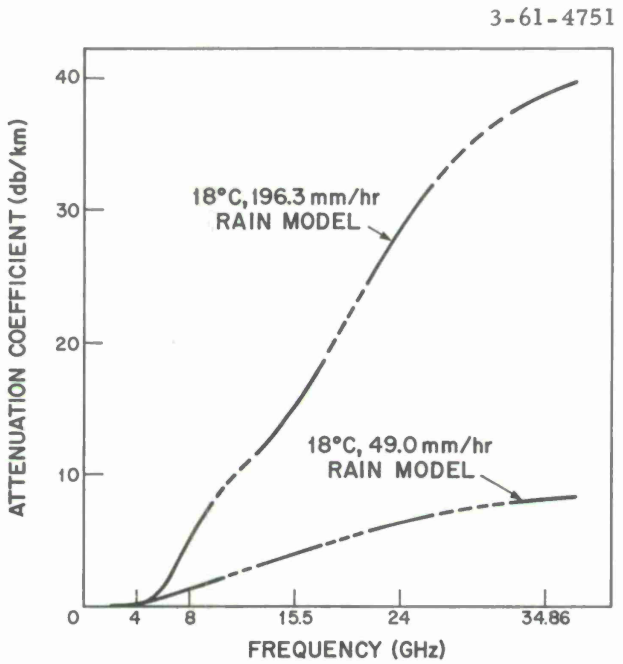

Fig. 3. Attenuation coefficient vs. frequency.

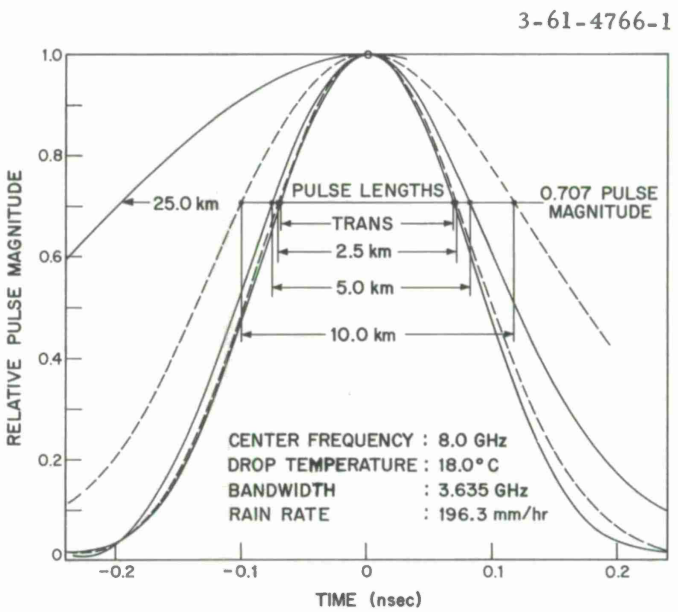

Fig. 4. Pulse magnitude vs. time.

3-61-4756

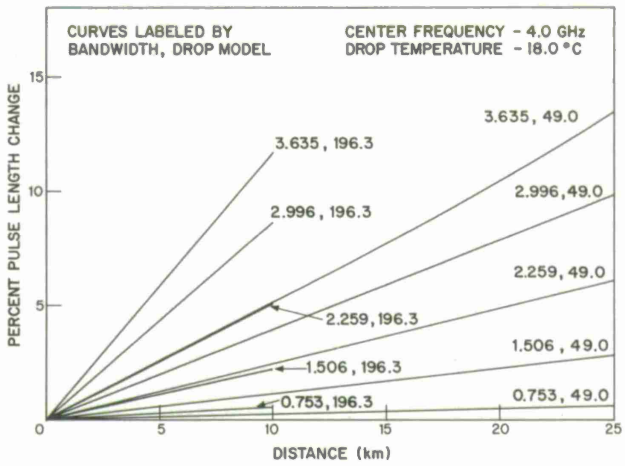

Fig. 5. Percent pulse length change vs. distance.

3-61-4755

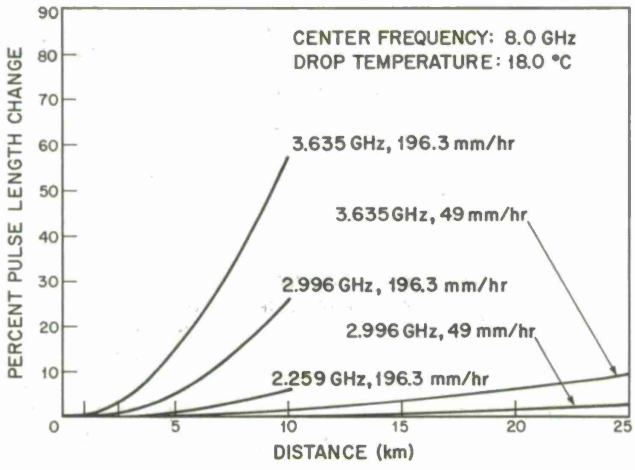

Fig. 6. Percent pulse length change vs. distance.

3-61-4765

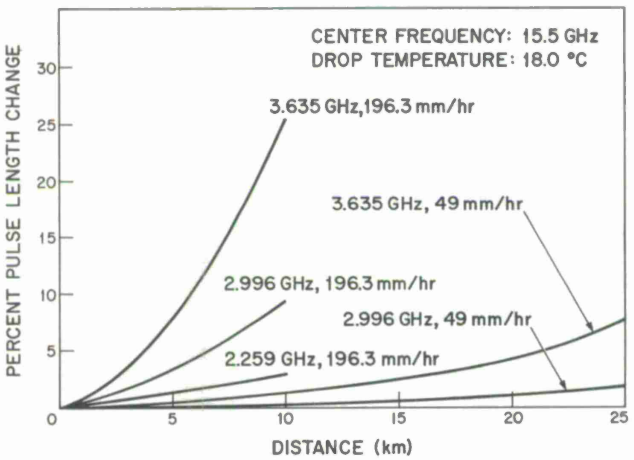

Fig. 7. Percent pulse length change vs. distance.

3-61-4757

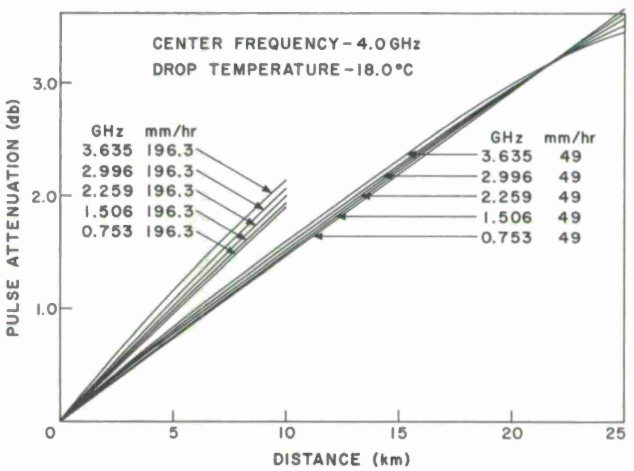

Fig. 8. Pulse attenuation vs. distance.

3-61-4758

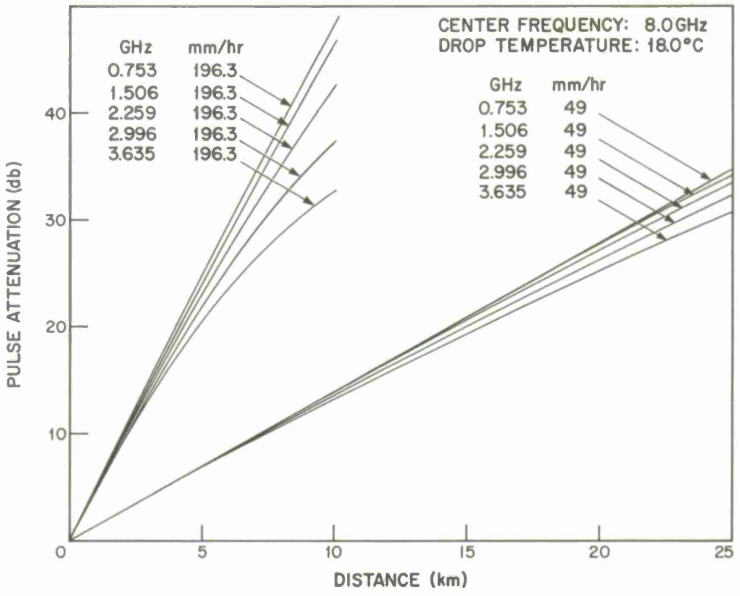

Fig. 9. Pulse attenuation vs. distance.

3-61-4764

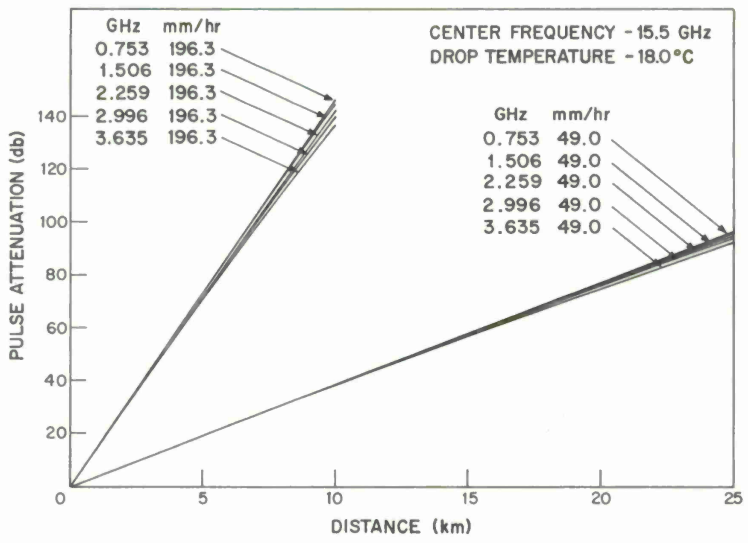

Fig. 10. Pulse attenuation vs. distance.

3-61-4753

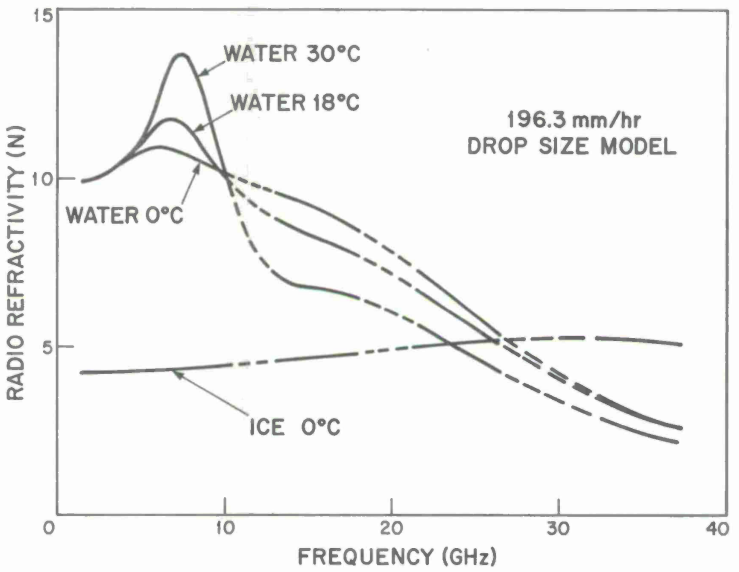

Fig. 11. Radio refractivity vs. frequency.

3-61-4752

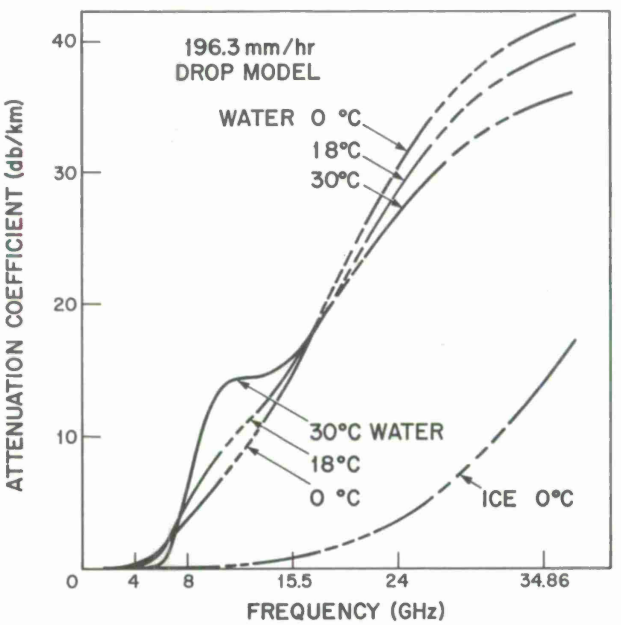

Fig. 12. Attenuation coefficient vs. frequency.

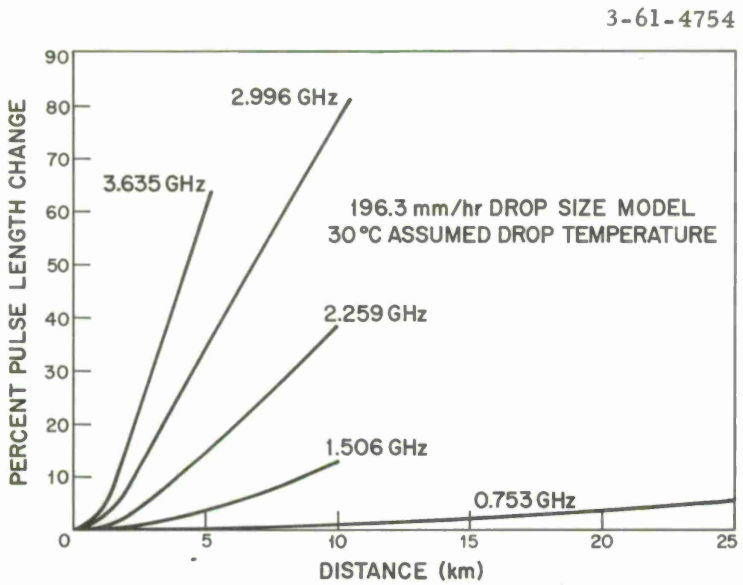

Fig. 13. Percent pulse length change vs. distance.

DISTRIBUTION LIST

Division 6

Morrow, W. E.
Rosen, P.
Gould, S.

Group 61

Ricardi, L. J.
Assaly, R. N.
Burns, R. J.
Burrows, M. L.
Crane, R. K.
Devane, M. E.
Dion, A.
Frediani, D. J.
LaPage, B. F.
Lindberg, C. A.
Niro, L.
Rankin, J. B.
Rosenthal, M. L.
Sotiropoulos, A.

Group 62

Lebow, I. L.
Drouilhet, P. R.
Jordan, K. L.
Nichols, B. E.
Lock, R. V.
Ploussios, G.
Rader, C. M.

Group 63

Sherman, H.
MacLellan, D. C.
Waldron, P.
Berg, R. S.
McCarron, J. D.
McMahon, R. E.
Michelove, L. D.
Parker, D.

Group 64

Green, P. E.
Briscoe, H. W.
Capon, J.
Fleck, P. L.

Group 65

Wood, R. V.
Enticknap, R. G.
Brown, J. R.
Densler, J. P.

Group 66

Reiffen, B.
Beusch, J. U.
Goblick, T. J.

Division 3

Chisholm, J. H.
Ruze, J.

Group 31

Sebring, P. B.
Pineo, V. C.
Stone, M. L.
Meeks, M. L.

Division 4

Weiss, H. G.

Group 46

Jones, C. W.
Keeping, K. J.
McCue, J. J. G.

Division 7

Hutzenlaub, J. F.

DISTRIBUTION LIST (Continued)

AFCRL

Falcone, V.
Kalaghan, P.
Wolfsberg, K.

M. I. T.

Austin, Dr. Pauline

MITRE

Kelly, George

Mr. Eugene A. Mueller
Illinois State Water Survey
Urbana, Illinois

Dr. Roger M. Lhermitte
National Severe Storms Laboratory
Norman, Oklahoma

Mr. James R. Poppe
General Electric Company
Mountain View Plant
Lynchburg, Virginia

Dr. Wolfgang Kummer
Research and Development Division
Aerospace Group
Hughes Aircraft Company
Culver City, California

Mr. Roy M. Dohoo
Defense Research Board
Shirley Bay
Ottawa, Canada

Lt. R. M. Price
AMSEL XL C
U. S. Army Electronics Command
Fort Monmouth, New Jersey

Mr. F. J. Altman
System Sciences Corporation
5718 Columbia Pike
Falls Church, Virginia 22041

DOCUMENT CONTROL DATA – R&D

(Security classification of title, body of abstract and indexing annotation must be entered when the overall report is classified)

1. ORIGINATING ACTIVITY *(Corporate author)* Lincoln Laboratory, M.I.T.	2a. REPORT SECURITY CLASSIFICATION Unclassified 2b. GROUP None

3. REPORT TITLE

Coherent Pulse Transmission Through Rain

4. DESCRIPTIVE NOTES *(Type of report and inclusive dates)*

Technical Note

5. AUTHOR(S) *(Last name, first name, initial)*

Crane, Robert K.

6. REPORT DATE 27 December 1966	7a. TOTAL NO. OF PAGES 34	7b. NO. OF REFS 3
8a. CONTRACT OR GRANT NO. AF 19(628)-5167 b. PROJECT NO. 649L c. d.	9a. ORIGINATOR'S REPORT NUMBER(S) Technical Note 1966-63 9b. OTHER REPORT NO(S) *(Any other numbers that may be assigned this report)* ESD-TR-66-601	

10. AVAILABILITY/LIMITATION NOTICES

Distribution of this document is unlimited.

11. SUPPLEMENTARY NOTES None	12. SPONSORING MILITARY ACTIVITY Air Force Systems Command, USAF

13. ABSTRACT

The problem of received signal degradation for coherent pulse transmission through a rain scattering volume was investigated for large bandwidth transmission at 4.0, 8.0, 15.5 and 34.86 GHz. Calculations of pulse length and total pulse energy were made for different path lengths through the rain volume. The calculations were made for models of heavy and extreme rainfall, using rain rates 49.0 and 196.3 mm/hr. The results of the computations show that for the rain rates considered, the dominant cause of signal degradation is attenuation. Negligible pulse lengthening was noted at 34.86 GHz. For rain rates above 196 mm/hr. and frequencies of 15.5 and 8.0 GHz, measurable values of pulse lengthening were calculated for bandwidths above 2.0 GHz. At 4.0 GHz, measurable values of pulse lengthening were obtained for both rain rates considered.

14. KEY WORDS

pulse transmission
rain
attenuation

Printed by
United States Air Force
L. G. Hanscom Field
Bedford, Massachusetts